

FABRICATION OF FLEXIBLE MULTILAYER TRANSPARENT ELECTRODE BASED ON SILVER NANOWIRE, GRAPHENE OXIDE, AND POLY(3,4-ETHYLENEDIOXYTHIOPHENE): POLYSTYRENE SULFONATE

Thi Thu Hien Nguyen^{1,4}, Minh Hoang Nguyen², Minh Triet Khong², Thi Kim Dung Nguyen², Tien Dat Doan¹, Nhung Hac Thi¹, Ho Thi Oanh¹, Nguyen Duc Tuyen¹, Dinh Long Phan³, Tuyen Van Nguyen¹, Mai Ha Hoang^{1,*}

¹*Institute of Chemistry, Vietnam Academy of Science and Technology, 18 Hoang Quoc Viet, Cau Giay, Ha Noi, Viet Nam*

²*Viet Yen 1 High School, Viet Yen, Bac Giang, Viet Nam*

³*College of Economics - Technology of Industry and Commerce, 569 Quang Trung, Thanh Hoa City, Thanh Hoa, Viet Nam*

⁴*Hanoi University of Science and Technology, 1 Dai Co Viet, Hai Ba Trung, Ha Noi, Viet Nam*

*Emails: hoangmaiha@ich.vast.vn

Received: 23 October 2021; Accepted for publication: 21 December 2021

Abstract. High-performance flexible multilayer transparent conducting electrodes (TCE) based on silver nanowires (AgNWs), graphene oxide (GO), and poly(3,4-ethylenedioxythiophene): polystyrene sulfonate (PEDOT:PSS) materials were successfully fabricated by spin-coating technique. The multilayer electrodes were fabricated using different combinations of AgNW, GO, and PEDOT:PSS materials. The morphological, physical properties, surface roughness, and durability of the fabricated electrodes were investigated. The results indicated that the five-layer structured electrode of PEDOT:PSS/GO/AgNW/GO/PEDOT:PSS possesses the best performance with a sheet resistance of 23 Ω /sq, transmittance of 85 %, and surface roughness of 8 nm. In addition, the PEDOT:PSS/GO/AgNW/GO/PEDOT:PSS electrode also exhibited high durability after being exposed to the environment for 30 days. The electrode can be used as a promising electrode in optoelectronic devices.

Keywords: Flexible transparent electrode, silver nanowire, graphene oxide, PEDOT:PSS.

Classification numbers: 2.1.3, 2.4.1, 2.5.2.

1. INTRODUCTION

Transparent conductive electrodes (TCEs) are one of the essential components which are used in various optoelectronic devices such as solar cells, organic light-emitting diodes (OLEDs), touch screens, etc. [1]. Indium tin oxide (ITO) is currently a common material to fabricate electrodes because of its advantages such as good electrical conductivity and high transmittance [2]. However, the use of ITO has several drawbacks, which are relatively high

cost, brittle nature, and scarcity of indium [3, 4]. Thereby, several materials such as graphene oxide, conductive polymers, metal nanowires, or metal-polymer hybrids have been studied as alternatives to ITO [5 - 8].

Among them, silver nanowires (AgNWs) have been considered a promising candidate because of its good electrical conductivity, outstanding transmittance, and high flexibility. However, several disadvantages were observed when using AgNWs to fabricate electrodes including weak adhesion to the substrate, high surface roughness, and low chemical stability [9]. To overcome these drawbacks, scientists have studied to combine AgNWs with other materials, such as graphene oxide (GO) and poly(3,4-ethylenedioxythiophene):polystyrene sulfonate (PEDOT:PSS) [10]. GO is a well-known derivative of graphene that possesses various unique properties such as good charge exchange, large surface area, and high mechanical strength [11]. Liang *et al.* used GO to improve the properties of the AgNWs electrode. The results showed that the AgNW/GO electrode owned good optical and electrical properties. Moreover, the electrode exhibited high durability because GO could shield AgNWs from the effects of the environment [12]. In addition, there have been several reports using PEDOT:PSS to improve the roughness surface as well as the conductivity of the AgNWs electrode [13, 14]. Therefore, the quality of the electrode may be improved by optimizing the structure based on AgNWs, GO, and PEDOT:PSS materials.

In this study, AgNWs electrode and multilayer structure electrodes were fabricated based on AgNWs, GO, and PEDOT:PSS materials by spin-coating technique. Because of the unique properties such as high transparency, good flexibility and excellent thermal stability, polyethylene terephthalate (PET) film was used as an electrode substrate. The electrical conductivity, transmittance, surface roughness, and stability in the environment of fabricated electrodes were investigated. The result indicated that the five-layer structured electrode of PEDOT:PSS/GO/AgNW/GO/PEDOT:PSS exhibited the best properties among the six fabricated electrode configurations.

2. MATERIALS AND METHODS

2.1. Materials

AgNO₃ 99.8 % and ethylene glycol (EG) 99 % were purchased from Fisher Scientific. Polyvinylpyrrolidone (PVP: M_w ~ 360000 gmol⁻¹); graphite (powder) < 20 μm; 3,4 ethylene dioxythiophen (EDOT) 97 %; poly 4-styrenesulfonic acid (PSS: M_w ~ 75000 gmol⁻¹); and PET substrate with dimensions of 300 mm × 300 mm, thickness of 0.25 mm were provided by Sigma-Aldrich. H₂SO₄, NaNO₃, KMnO₄, H₂O₂, Na₂S₂O₈, FeSO₄·7H₂O, isopropanol (IPA) and HCl were of high purity and were used directly without further purification.

2.2. Synthesis of AgNWs, GO, and PEDOT:PSS materials

AgNWs were synthesized by polyol method using AgNO₃ as a precursor and EG acting both as a solvent and reducing agent [15]. GO was synthesized by the Hummers method [16] using graphite (precursor), NaNO₃, H₂SO₄, and KMnO₄ as an oxidizing agent. PEDOT:PSS was synthesized by oxidative polymerization of EDOT with Na₂S₂O₈ as an oxidizing agent and FeSO₄ as a catalyst [17]. Specifically, PSS (2.82 g) was mixed in 250 mL of water containing 0.98 % of Na₂S₂O₈ and 0.2 % of FeSO₄·7H₂O. Then, 0.38 mL of HCl was added and the mixture was stirred at 20 °C for 30 min. Thereafter, EDOT (2.18 g) was added, followed by continued stirring for 24 hours. After polymerization, the Na⁺, Fe²⁺, and SO₄²⁻ ions were removed by ion

exchange method. The PEDOT:PSS product was washed and dispersed in water to create a dark blue solution with a concentration of 1.3 %.

2.3. Fabrication of transparent electrode based on AgNWs, GO, and PEDOT:PSS materials

In this study, we fabricated six different electrode structures (Figure 1). PET substrates (2.5 cm × 2.5 cm) were ultrasonically washed twice with deionized water and IPA for 10 min [18, 19]. The substrate was then dried with a nitrogen gun and left in an oven at 80 °C for 15 min. To fabricate different electrode configurations, three solutions of AgNWs, GO and PEDOT:PSS were coated onto a PET substrate by spin-coating method at 2000 rpm for 40 s. Thereafter, these electrodes were dried at 120 °C for 5 min.

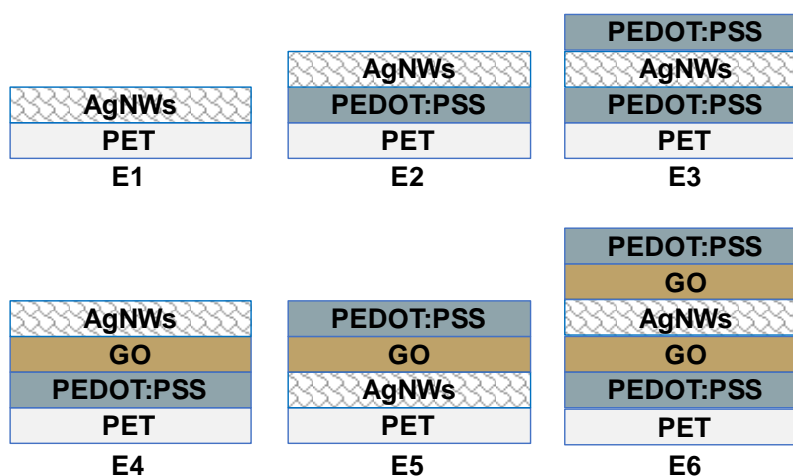


Figure 1. Six different electrodes based on AgNWs, GO, and PEDOT:PSS materials.

2.4. Characterization

The morphology of the materials was observed by field emission scanning electron microscopy (FE-SEM) (Hitachi S-4800) and transmission electron microscopy (TEM) (JOEL JEM1010). Fourier transform infrared (FT-IR) spectra were obtained in the range of 450 - 4000 cm^{-1} by a PerkinElmer FT-IR spectrometer. The X-ray diffraction (XRD) patterns were investigated using a D8 ADVANCE instrument (Bruker) with Cu-K_α radiation ($\lambda = 1.5406 \text{ \AA}$). The zeta potential was measured with an Anton Paar Litesizer 500 using a dynamic light scattering (DLS) technique. The transmittance of these electrodes was investigated using a UV-vis absorption spectrometer (SP-3000 nano) with $\lambda = 190 - 1100 \text{ nm}$. The sheet resistance of the electrodes was measured with a four-point probe (Jandel RM3000). The surface morphology of transparent electrodes was studied using an atomic force microscope (XE-100).

3. RESULTS AND DISCUSSION

3.1. Properties of materials

The morphology of AgNWs were observed by field-emission scanning electron microscopy, and the results are shown in Figure 2a-b. The synthesized AgNWs had a mean

diameter of 35 nm and length of 20 μm . To fabricate electrodes, AgNWs were dispersed in IPA solvent at a concentration of 0.4 %.

The morphology of GO was observed using transmission electron microscopy (Figure 2c). The GO layer is very thin with high transparency. As shown in Figure 2d, the average zeta potential of GO is about -33 mV. This negative value shows a highly stable dispersion of GO in water. The synthesized GO was dispersed in water with a concentration of 0.05 %.

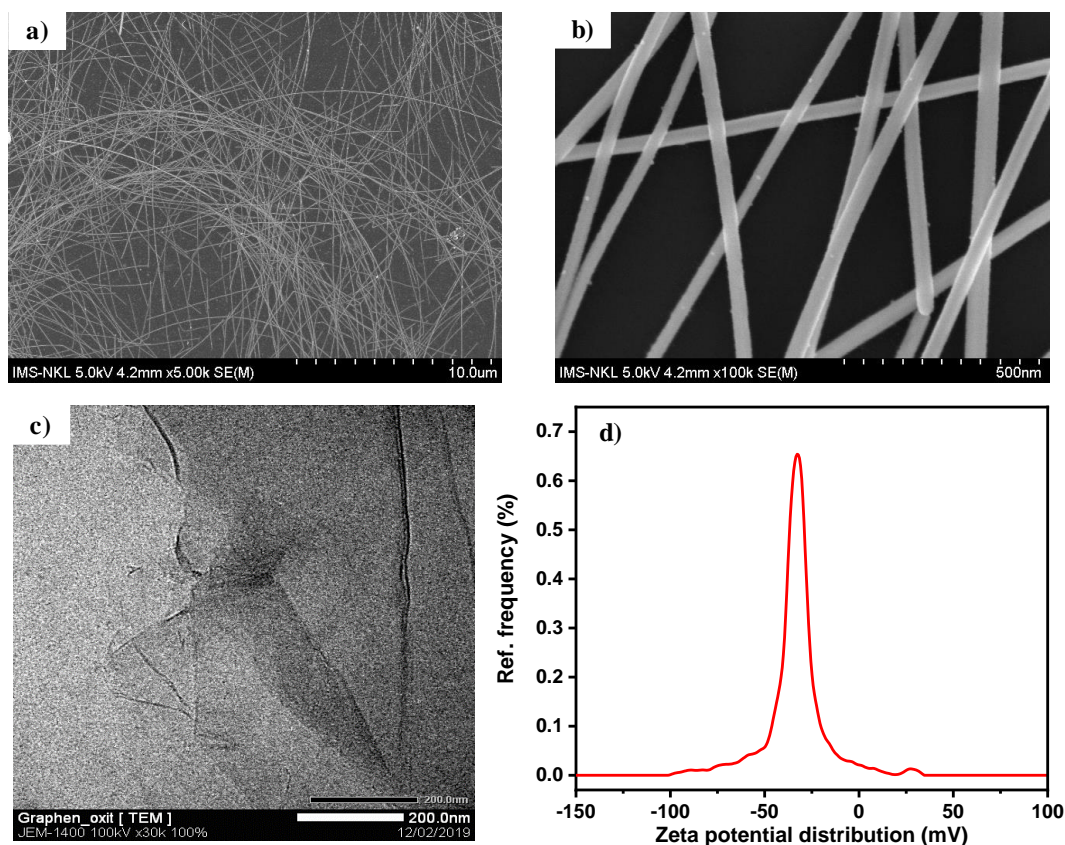


Figure 2. The morphology of AgNWs (a,b), GO (c), and the zeta potential of GO (d).

The composition of the electrodes was studied by X-ray diffraction (Figure 3a). The XRD pattern of the AgNW/GO electrode exhibits 4 diffraction peaks of silver metal at positions 38.12° , 44.11° , 64.55° , and 77.26° corresponding to (111), (200), (220), and (311) planes, respectively, (JCPDS card No. 04-0783). These diffraction peaks verify the presence of AgNWs in the AgNW/GO electrode. Besides, there is a peak at $2\theta = 11^\circ$, which is relatively consistent with the (001) plane of GO.

Figure 3b exhibits the FT-IR spectra of AgNWs, GO, PEDOT:PSS, and AgNW/GO/PEDOT:PSS film. In the FT-IR spectrum of AgNWs, there appear absorption bands at $2700 - 3300$, $165 - 1670$, $1050 - 1250$, $1020 - 1230 \text{ cm}^{-1}$ corresponding to stretching vibrations of C-H, C=O, C-O, and C-N, respectively, because of the presence of PVP surfactant [20]. The FT-IR spectrum of graphene oxide exhibits the characteristic bands of GO at 3420 , 1720 , 1180 cm^{-1} which are attributed to the -OH group, C=O group, and epoxy group, respectively [21]. For the spectrum of PEDOT:PSS, two peaks at 1398 and 1631 cm^{-1} are attributed to the stretching

vibrations of the C-C and C=C bonds on the thiophene ring. The peaks at 1093 and 1130 cm^{-1} are caused by stretching vibrations of the C-O-C of the ether group on the EDOT. The peak at 820-980 cm^{-1} is caused by the vibration mode of the C-S bonds [22]. The peak at 670 cm^{-1} is attributed to the stretching vibration of the S=O group of the PSS [23]. In addition, the characteristic peaks of AgNWs, GO and PEDOT:PSS also appear on the FT-IR spectrum of AgNW/GO/PEDOT:PSS film.

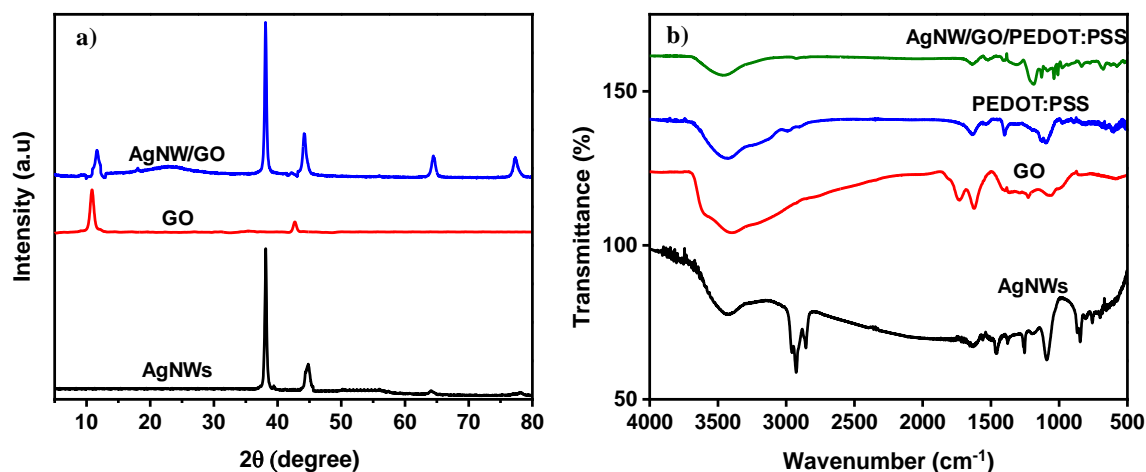


Figure 3. XRD patterns of AgNWs, GO and AgNW/GO (a); FT-IR spectra of AgNWs, GO, PEDOT:PSS, and AgNW/GO/PEDOT:PSS (b).

3.2. Surface morphology of electrodes

The surface morphology of six electrodes were observed by field emission scanning electron microscopy (Figure 4). For electrodes E1 and E5, AgNWs are unevenly distributed on the electrode surface due to the poor hydrophilicity of the PET substrate and the weak adhesion of AgNWs to the substrate surface. Thereby, AgNWs will be thrown off until getting engaged by each other during the spin-coating process. For the other electrodes, AgNWs were coated onto GO or PEDOT:PSS buffer layer; thus, AgNWs were more uniformly dispersed on the PET substrate. Because the GO and PEDOT:PSS buffer layer enhanced the dispersion and spreading ability of the AgNWs solution, the distribution of AgNWs on the PET surface was improved.

Surface roughness is an important factor for applying transparent electrodes on optoelectronic devices. To find a quality-assured electrode, we investigated the surface roughness of six electrodes by atomic force microscopy and the result was shown in Figure 5. Electrode E1 exhibited the highest surface roughness with the R_q of 36 nm due to the random overlapping between AgNWs. In addition, the uneven distribution of AgNWs on the surface of PET substrate also caused large surface roughness of the electrode. In the case of electrodes E2, E3, E4, and E6, because of the presence of GO or PEDOT:PSS buffer layer, the AgNWs were more evenly dispersed, thereby improving the surface roughness of these electrodes. For electrodes E5 and E6, AgNWs are coated by GO and PEDOT:PSS layers; thus, the shape of the individual AgNWs is not clearly observed. This is consistent with the observations from the SEM images (Figure 4). Electrode E6 owns a surface roughness with R_q value of 8 nm, which is the lowest value of six electrodes. Because of coating GO on AgNWs layer, GO tightly pressed the AgNWs to the substrate. Besides, the PEDOT:PSS layer above also reduced the electrode's surface roughness. The R_q value of electrode E6 is lower than that of the electrode which coats

only one GO layer or one PEDOT:PSS layer on AgNWs electrode in the previous studies [14,24]. Therefore, by using the five-layer structure PEDOT:PSS/GO/AgNW/GO/ PEDOT:PSS, the surface roughness, which was a drawback of the AgNWs electrode, was significantly improved with the low Rq value of 8 nm.

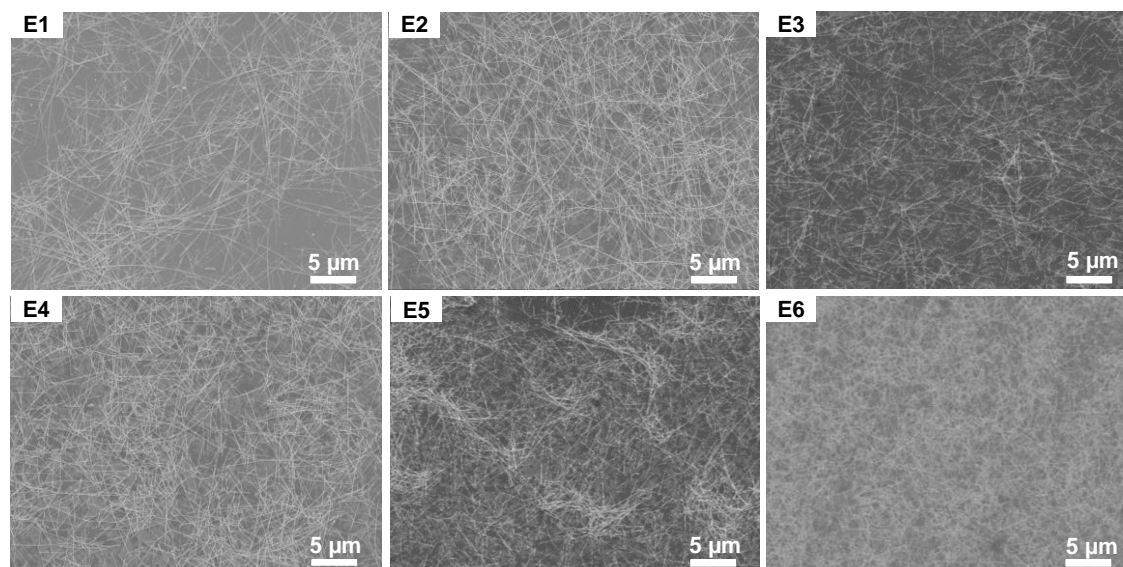


Figure 4. SEM images of six electrodes.

3.3. Properties of electrodes

Transmittance and electrical conductivity are important properties for evaluating transparent electrodes. The transmission spectra of the fabricated electrodes were studied using a UV-Vis absorption spectrometer (Figure 6a). The sheet resistance of these electrodes was determined by four-probe resistance measurement. Table 1 illustrates the results of the transmittance and the sheet resistance of six electrodes.

Table 1. The transmittance and sheet resistance of electrodes based on AgNWs, GO, and PEDOT:PSS materials.

Electrode (on PET)	Sheet resistance (Ω/sq)	Transmittance (%)	FoM ($\times 1000$)	Surface roughness (nm)
E1	43	87	5.7	36
E2	35	88	8.0	32
E3	30	87	8.3	20
E4	32	86	6.9	28
E5	28	84	6.2	15
E6	23	85	8.6	8

For electrode E1, because of the thermal annealing, the sheet resistance was reduced from 120 Ω/sq to 43 Ω/sq . The resistance value of electrode E1 is relatively high among the six electrodes. This is because of the uneven dispersion of AgNWs on the PET substrate (Figure 4a). Besides, the weak adhesion of AgNWs to the substrate surface [25] leads to a high value of sheet resistance. For electrodes E2 and E4, the PEDOT:PSS or GO buffer layer helped to improve the

adhesion of AgNWs; thus, the sheet resistance of these electrodes were lower than that of electrode E1. In the case of electrode E3, the AgNWs layer was inserted between two layers of PEDOT:PSS, the resistance of this electrode was reduced to a low value of $30 \Omega/\text{sq}$. The sheet resistance of this electrode was improved because PEDOT:PSS layer played the role of charge transport in the space in the AgNWs network structure. For electrodes E5 and E6, the GO layer compressed the AgNWs onto the electrode surface, thereby improving the junction between the AgNWs [26]. This accounts for the lower sheet resistance of electrodes E5 and E6 compared to other electrodes. In which, electrode E6 owned the lowest sheet resistance with a value of $23 \Omega/\text{sq}$.

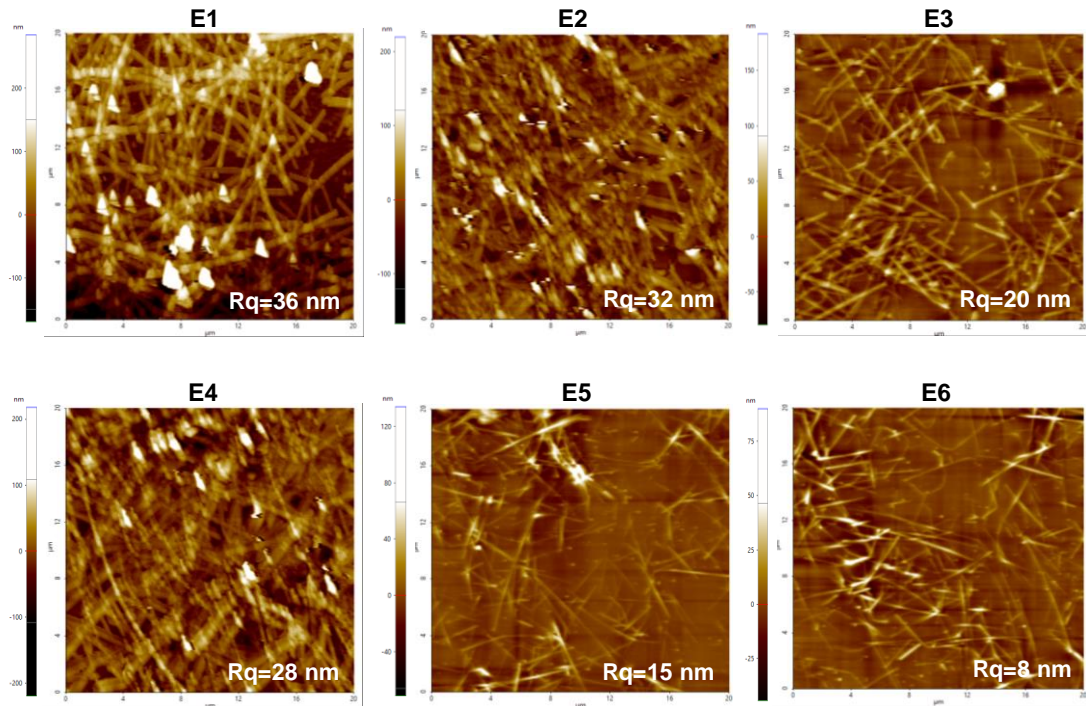


Figure 5. AFM images of six fabricated electrodes.

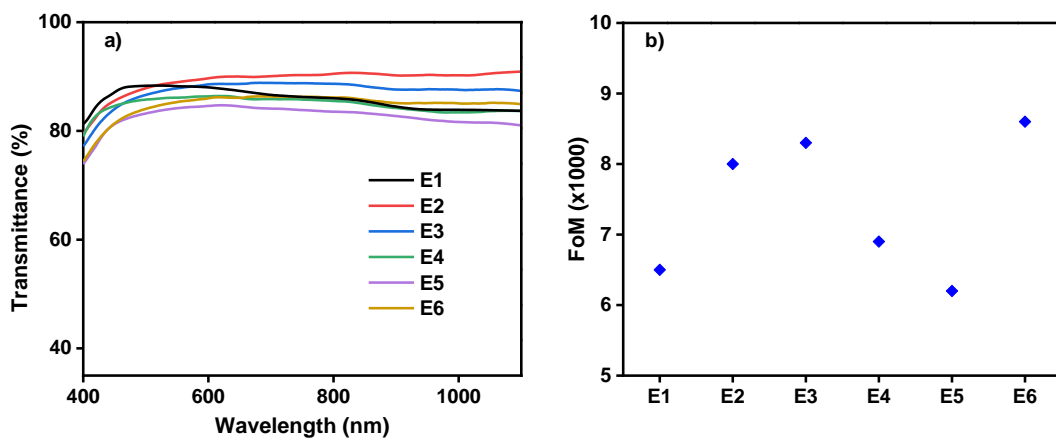


Figure 6. The transmittance (a) and the FoM value (b) of six fabricated electrodes.

Figure 6a illustrates the transmittance of these fabricated electrodes. The results showed that the transmittance of all electrodes are higher than 80 % at 550 nm. In which, electrode E2 possessed the best transmittance of 88 %. Although electrode E2 owned a two-layer structure, the PEDOT:PSS bottom layer helped to improve the dispersion of AgNWs; thus, the transmittance of electrode E2 was better than that of electrode E1. For electrodes E3 and E4, due to the coating of PEDOT:PSS top layer (electrode E3) or GO bottom layer (E4), the transmittance of these electrodes was slightly reduced. The transmittance of electrodes E3 and E4 possessed values of 87 % and 86 %, respectively. In comparison with electrode E5, despite electrode E6 had a five-layer structure, the transmittance of this electrode was better because GO and PEDOT:PSS buffer layer improved the distribution of AgNWs on the PET surface.

To optimize the optical and electrical properties, and find the best quality electrode, we calculated the FoM value of six electrodes (Figure 6b). The FoM values of these electrodes are calculated according to the following formula:

$$FoM = \frac{T^{10}}{R}$$

where T is the transmittance at 550 nm; R is the sheet resistance.

The results illustrated that electrode E6 owned the highest FoM value of 8.6. The obtained value is slightly higher than the previously published values [10, 13, 14]. This value is even equivalent to the FoM of a commercial ITO electrode [14]. Based on the results of the transmittance and the sheet resistance, it can be concluded that the PEDOT:PSS/GO/AgNW/GO/PEDOT:PSS electrode (electrode E6) exhibited the best performance to apply in optoelectronic devices.

3.4. Stability of electrodes

Stability is an important property for the practical application of transparent electrodes. The stability of these electrodes was investigated by measuring the sheet resistance during 30 days of storage under ambient conditions. The results of the stability of the electrodes are shown in Figure 7.

Figure 7a shows that the sheet resistance of the electrodes increased gradually after 30 days of storage under ambient conditions. Meanwhile, the transmittance of these electrodes changed negligibly (Figure 7b). Electrodes E2 and E3 exhibited a large increase in sheet resistance because of the acidity of PEDOT:PSS causing the corrosion of AgNWs. In addition, PEDOT:PSS owned hygroscopic nature therefore its conductivity was also reduced after 30 days. For electrode E1, although the AgNWs were not exposed to the PEDOT:PSS layer, AgNWs were directly oxidized by environmental agents such as oxygen, UV light and humidity. Thereby the resistance of this electrode also increased by 16 % after 30 days. In the case of electrode E4, the GO buffer layer helped to minimize the impact of the acidity of PEDOT:PSS on AgNWs. However, similar to electrode E1, the sheet resistance of electrode E4 significantly increased because this electrode was also affected by oxidizing effects from the environment. Unlike other electrodes, the resistance of electrodes E5 and E6 increased more slowly. The coating of GO on AgNWs as a protective layer shielded the AgNWs from the effects of the environment as well as the corrosive effects of PEDOT:PSS. In addition, the GO film also restrained the impact of humidity on the AgNWs electrode. Therefore, the use of the GO layer to fabricate electrodes improved the stability of the electrodes.

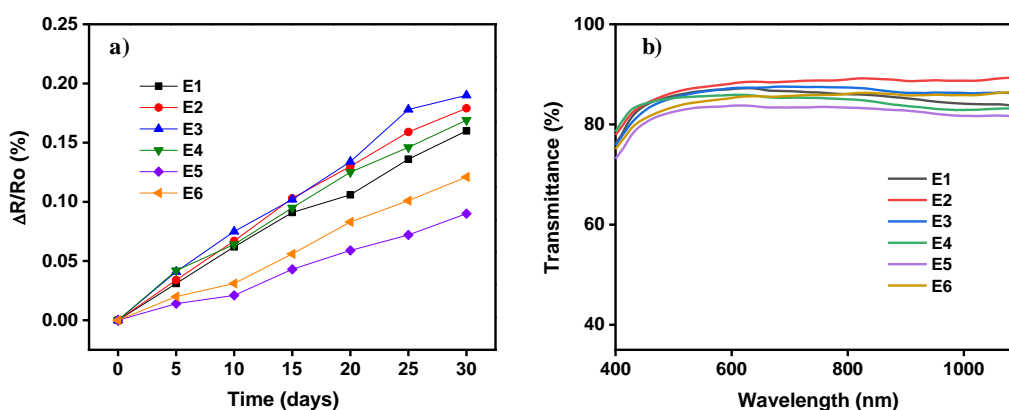


Figure 7. Changes in the sheet resistance (a) and the transmittance (b) of six electrodes.

4. CONCLUSION

Transparent flexible electrodes based on AgNWs, GO and PEDOT:PSS materials were successfully fabricated by spin-coating method. Among them, the PEDOT:PSS/GO/AgNW/GO/PEDOT:PSS electrode exhibited excellent optical and electrical properties with a low resistance of 23 (Ω/sq) and high transmittance of 85 %. In addition, the five-layer structured electrode possessed a surface roughness of only 8 nm, which was the lowest value among the investigated electrodes. Besides, this electrode also displayed high stability after 30 days of storage under ambient conditions. The combination of AgNWs, GO, and PEDOT: PSS into the five-layer structured electrode could improve the drawbacks of these materials. This structure can be applied for the fabrication of transparent flexible electrodes to use in optoelectronic devices.

Acknowledgement. This research is funded by the Ministry of Science and Technology of Viet Nam under grant number “NDT.42.KR/18”.

CRedit authorship contribution statement. Thi Thu Hien Nguyen, Minh Hoang Nguyen, Minh Triet Khong, Thi Kim Dung Nguyen, Tien Dat Doan: Synthesis of materials; Nhung Hac Thi, Ho Thi Oanh: Performing measurements (UV-Vis, AFM, FT-IR, XRD, sheet resistance); Nguyen Duc Tuyen, Dinh Long Phan: Performing analysis and assessment of morphology; Thi Thu Hien Nguyen: Writing original draft; Tuyen Van Nguyen, Mai Ha Hoang: Supervision, review & editing.

Declaration of competing interest. The authors declare that they have no known competing financial interests or personal relationships that could have appeared to influence the work reported in this paper.

REFERENCES

1. Jinhong D., Songfeng P., Laipeng M., Hui M. C. - 25th anniversary article: Carbon nanotube- and graphene-based transparent conductive films for optoelectronic devices, *Adv. Mater* **26** (2014) 1958-1991. <https://doi.org/10.1002/adma.201304135>.
2. Shengrong Y., Aaron R. R., Zuofeng C., Ian E. S., Benjamin J. W. - Metal nanowire networks: The next generation of transparent conductors, *Adv. Mater* **26** (2014) 6670-6687. <https://doi.org/10.1002/adma.201402710>.
3. Seok I. N., Seok S. K., Jang J., Dong Y. K. - Efficient and flexible ITO-free organic solar cells using highly conductive polymer anodes, *Adv. Mater* **20** (2008) 4061-4067. <https://doi.org/10.1002/adma.200800338>.

4. Churl S. L., Joung E. Y., Kwonwoo S., Park C. O., Joonho B. - Carbon nanotube-silver nanowire composite networks on flexible substrates: high reliability and application for supercapacitor electrodes, *Phys. Status Solidi A* **211** (2014) 2890-2897. <https://doi.org/10.1002/pssa.201431538>.
5. Zongyou Y., Shuangyong S., Teddy S., Shixin W., Xiao H., Qiyuan H., Yeng M. L., Hua Z. - Organic photovoltaic devices using highly flexible reduced graphene oxide films as transparent electrodes, *ACS Nano* **4** (2010) 5263-5268. <https://doi.org/10.1021/nn1015874>.
6. Youn S. K., Eun J. L., Jun T. L., Do K. H., Won K. C., Jin Y. K. - High-performance flexible transparent electrodes films based on silver nanowire-PEDOT:PSS hybrid-gels, *RSC Adv* **6** (2016) 64428-64433. <https://doi.org/10.1039/C6RA06590B>.
7. Zhuang C. W., Zhihong. C., Xu D., Jonathan M. L., Jennifer S., Maria N., Katalin K., John R. R., David B. T., Arthur F. H., Andrew G. R. - Transparent, conductive carbon nanotube films, *Science* **305** (2004) 1273-1276. <https://doi.org/10.1126/science.1101243>.
8. Chunxiong B., Jie Y., Hao G., Faming L., Yingfang Y., Bo Y., Gao F., Xiaoxin Z., Tao Y., Yiqiang Q., Jianguo L., Zhigang Z. - In situ fabrication of highly conductive metal nanowire networks with high transmittance from deep-ultraviolet to near-infrared, *ACS Nano* **9** (2015) 2502-2509. <https://doi.org/10.1021/nn504932e>.
9. Daniel L., Gael G., Celine M., Caroline C., Daniel B., Jean P. S. - Flexible transparent conductive materials based on silver nanowire networks: a review, *Nanotechnology* **24** (2013) 452001. <https://doi.org/10.1088/0957-4484/24/45/452001>.
10. Yasin A., Mahmut T., İsmail B., Ali D., Ayse B. - Solution-processed transparent conducting electrodes with graphene, silver nanowires and PEDOT:PSS as alternative to ITO, *Surface & Coatings Technology* **302** (2016) 75-81. <https://doi.org/10.1016/j.surfcoat.2016.05.058>.
11. Pham T. T., Le V. T., Tran V. K., Tran X. D., Chau N. T. N., Tran T. T. N., Le M. T., Nguyen N. V., Nguyen M. H. - Synthesis of Ag/GO nanocomposite with promising photocatalytic ability for reduction reaction of p-nitrophenol, *Mater. Res. Express* **8** (2021) 105009. <https://doi.org/10.1088/2053-1591/ac2ead>.
12. Jiajie L., Lu L., Kwing T., Zhi R., Wei H., Xiaofan N., Yongsheng C., Qibing P. - Silver nanowire percolation network soldered with graphene oxide at room temperature and its application for fully stretchable polymer light-emitting diodes, *ACS nano* **8** (2014) 1590-1600. <https://doi.org/10.1021/nn405887k>.
13. Jinhwan L., Phillip L., Ha B. L., Sukjoon H., Inhwa L., Junyeob Y., Seung S. L., Taek S. K., Dongjin L., Seung H. K. - Room-temperature nanosoldering of a very long metal nanowire network by conducting-polymer-assisted joining for a flexible touchpanel application, *Adv. Funct. Mater* **23** (2013) 4171-4176. <https://doi.org/10.1002/adfm.201203802>.
14. Young U. K., Su H. P., Nguyen T. N., Mai H. H., Min J. C., Dong H. C. - Optimal Design of PEDOT:PSS Polymer-Based Silver Nanowire Electrodes for realization of Flexible Polymer Solar Cells, *Macromolecular Research* **29** (2021) 75-81. <https://doi.org/10.1007/s13233-021-9005-8>.
15. Nguyen T. N., Pham D. L., Doan T. D., Min J. C., Dong H. C., Hoang M. H. - Optimization of silver nanowire synthesis for flexible transparent conductive electrodes, *Vietnam J. Chem* **59** (1) (2021) 98-105. <https://doi.org/10.1002/vjch.202000131>.

16. Ayrat M. D., James M. T. - Mechanism of graphene oxide formation, *ACS Nano* **8** (3) (2014) 3060-3068. <https://doi.org/10.1021/nm500606a>.
17. Syang-Peng R., Yi-Huan L., Jia-Wei S., Ragu S., Uin-Ting S. -Characterization of Solvent-Treated PEDOT:PSS Thin Films with Enhanced Conductivities, *Polymers* **11** (134) (2019) 1-10. <http://doi.org/10.3390/polym11010134>.
18. Mohsin A., Mieke B., Wim D., Naveen R., Roos P. - Oxygen Gas and UV Barrier Properties of Nano-ZnO-Coated PET and PHBHHx Materials Fabricated by Ultrasonic Spray-Coating Technique, *Nanomaterials*. **11** (2021) 449. <https://doi.org/10.3390/nano11020449>.
19. Jun W., Jinting J., Teppei A., Masaya N., Tohru S., Shijo N., Hirotaka K., Peng H., Katsuki S. - Silver Nanowire Electrodes: Conductivity Improvement Without Post-treatment and Application in Capacitive Pressure Sensors, *Nanomicro Lett.* **7** (2015) 51-58. <https://doi.org/10.1007/s40820-014-0018-0>.
20. Hongshui W., Xueliang Q., Jianguo C., Xiaojian W., Shiyuan D. - Mechanisms of PVP in the preparation of silver nanoparticles, *Mater. Chem. Phys.* **94** (2005) 449-453. <https://doi.org/10.1016/j.matchemphys.2005.05.005>.
21. Long Z., Jiajie L., Yi H., Yanfeng M., Yan W., Yongsheng C. - Size-controlled synthesis of graphene oxide sheets on a large scale using chemical exfoliation, *Carbon N. Y.* **47** (2009) 3365-3368. <http://doi.org/10.1016/j.carbon.2009.07.045>.
22. Merih Z. Ç., Pinar C. - An amperometric glucose biosensor based on PEDOT PEDOT nanofiber, *RSC Adv.* **8** (2018) 19724–19731. <https://doi.org/10.1039/C8RA01385C>.
23. Yuan L., Nanlong H., An efficient hole transport material based on PEDOT dispersed with lignosulfonate: preparation, characterization and performance in polymer solar cells, *J. Mater. Chem. A.* **3** (2015) 21537-21544. <https://doi.org/10.1039/C5TA05167C>.
24. Neng Y., Jieli Y., Shuang X., Yuhua K., Tao L., Hongzheng C., Mingsheng X. - Silver nanowires-graphene hybrid transparent conductive electrodes for highly efficient inverted organic solar cells, *Nanotechnology* **28** (2017) 305402. <https://doi.org/10.1088/1361-6528/aa7723>.
25. Hui X., Xing Y., Dexi D., Yuzhen Z., and Yuehui W. - Flexible transparent conductive film based on random networks of silver nanowires, *Micromachines* **9** (2018) 295. <https://doi.org/10.3390/mi9060295>.
26. Byung Y. W., Eung S. L., Young J. O., Hyun W. K. - A silver nanowire mesh overcoated protection layer with graphene oxide as a transparent electrode for flexible organic solar cells, *RSC Adv.* **7** (2017) 52914-52922. <https://doi.org/10.1039/C7RA10889C>.